Palm Phytoliths of Mid-Elevation Andean Forests

Seringe N. Huisman, M. F. Raczka and Crystal N. H. McMichael*

Department of Ecosystem and Landscape Dynamics, Institute for Biodiversity and Ecosystem Dynamics, University of Amsterdam, Amsterdam, Netherlands

Palms are one of the most common tropical plant groups. They are widespread across lowland tropical forests, but many are found in higher altitudes have more constrained environmental ranges. The limited range of these species makes them particularly useful in paleoecological and paleoclimate reconstructions. Palms produce phytoliths, or silica structures, which are found in their vegetative parts (e.g., wood, leaves, etc.). Recent research has shown that several palms in the lowland tropical forests produce phytoliths that are diagnostic to the sub-family or genus-level. Here we characterize Andean palm phytoliths, and determine whether many of these species can also be identified by their silica structures. All of our sampled Andean palm species produced phytoliths, and we were able to characterize several previously unclassified morphotypes. Some species contained unique phytoliths that did not occur in other species, particularly *Ceroxylon alpinium,* which is indicative of specific climatic conditions. The differences in the morphologies of the Andean species indicate that palm phytolith analysis is particularly useful in paleoecological reconstructions. Future phytolith analyses will allow researchers to track how these palm species with limited environmental ranges have migrated up and down the Andean slopes as a result of past climatic change. The phytolith analyses can track local-scale vegetation dynamics, whereas pollen, which is commonly used in paleoecological reconstructions, reflects regional-scale vegetation change.

Keywords: Andean ecosystems, Arecaceae, *Ceroxylon*, *Dictyocaryum*, paleoecology, palms, phytoliths

INTRODUCTION

Arecaceae (palms) is a family of monocotyledonous plants that are important components of tropical ecosystems (Kahn and Mejia, 1990; Henderson et al., 1997; Phillips and Miller, 2002; Kahn and De Granville, 2012). Many palm species are widely distributed in the Neotropics, and belong to the most commonly found plants in Amazonian rainforests (Pitman et al., 2001; Vormisto et al., 2004; ter Steege et al., 2013). Many palms are also economically important for people, both in the modern era and in the past (Smith, 2014). Some of the earliest archaeological sites in the Andes and the Amazon contain evidence of a wide variety of palms consumed by people (Morcote-Rios and Bernal, 2001; Gnecco, 2003; Mora and Camargo, 2003). Some palm species, however, have constrained environmental tolerances or tend to be quite rare in the landscape, particularly in the mid-elevation regions (i.e., 1,000–3,000 m above sea level, hereafter masl) along the eastern Andean flank (Moraes et al., 1995; Henderson et al., 1997). Because the specific environmental optima vary between Andean palm species, palms are also important indicators of past climatic and ecosystem change in palaeoecological records (Bush et al., 2005, 2011; Schiferl et al., 2017); (Huisman et al., in revision).

Phytoliths are silica microfossils produced by many plant groups that can preserve in soils and lake sediments for millions of years (e.g., Strömberg, 2004; Piperno and Sues, 2005; Prasad et al., 2005; Piperno, 2006; Strömberg and McInerney, 2011). Phytoliths are commonly used in paleoecological and archaeological reconstructions, and provide evidence of local-scale vegetation dynamics because they are typically deposited directly beneath the parent plant when it dies and decays (Piperno, 2006). Palms are known to be particularly prolific phytolith producers, and can often be identified to the sub-family or genus level (Piperno, 2006; Morcote-Ríos et al., 2016).

There have been recent advances in the ability to identify palm phytoliths in tropical settings, particularly in the Amazonian lowland forests, and in an archaeological context (Morcote-Ríos et al., 2016). The phytoliths of Andean palm species, however, remain relatively unstudied. Most palaeoecological reconstructions of climatic change in Andean systems use pollen, which can travel >10 km from the source plant. Thus, the ability to identify phytoliths of Andean palms with narrow environmental ranges would be highly advantageous in generating local-scale reconstructions of past climatic change in Andean systems. Here, we characterize the phytolith morphology of 12 species of Andean palms using herbarium specimens, to provide a foundation for future paleoecological and archaeological reconstructions in these highly diverse and vulnerable ecosystems.

METHODS

We collected herbarium species of Andean palm species from the Naturalis Herbarium in Leiden, The Netherlands. We obtained leaves, seeds, wood, and flowers (based on availability) of 12 palm species known to occur in mid-elevation Andean forests from 1,000 to 3,000 masl (Moraes et al., 1995; Henderson et al., 1997; Table 1). If the Andean species were unavailable, other available species within the same genus were collected (Table 1).

Prior to preparation, the dry plant material was ground and heated to 450°C for 10 h. The samples were prepared by soaking in 33% hydrogen peroxide (H_2O_2), followed by 10% hydrochloric acid (HCl), and then potassium manganate ($KMnO_4$) to break down the organic material. They were mounted in Naphrax and heated on a boiling plate to stabilize the material.

All samples were analyzed under a Leica Axiophot microscope with differential interference contrast (DIC) at 630x magnification using immersion oil. Categorization was based on Morcote-Ríos et al. (2016), but new (sub)categories were created for newly identified morphotypes. A total of 300 phytoliths was counted per sample to quantify the relative abundances of morphotypes. At least 30 phytoliths were measured per morphotype to obtain size ranges. Phytoliths were photographed using a Fujifilm X-E2 camera and Zeiss Universal microscope (DIC, Plan-Neofluar 63/1.4) and edited in Adobe Lightroom CC, Adobe Photoshop CC, CorelDraw and Helicon Focus.

TABLE 1 | Herbarium material sampled from palm species occurring on the eastern Andean flank between 1,000 and 3,000 m above sea level (masl).

	Leaf	Seed	Wood	Flower
TRIBE CEROXYLEAE				
Ceroxylon alpinum Bonpl. ex DC.	x	x	x	
TRIBE CHAMAEDOREEAE				
Chamaedorea pinnatifrons (Jacq.) Oerst.	x			
TRIBE COCOSEAE				
Subtribe Bactridinae				
Aiphanes aculeata Willd.			x	
Bactris simpliciformis Mart.	x			
Subtribe Euterpeae				
Euterpe precatoria Mart.	x	x	x	
Euterpe catinga Wallace	x			
Hyospathe elegans Mart.	x			
Subtribe Geonomateae				
Geonoma paradoxa Burret	x			
Geonoma undata Klotzsch	x		x	
TRIBE IRIARTEEAE				
Dictyocaryum fuscum (H. Karst.) H. Wendl.	x	x		
Iriartea deltoidea Ruiz & Pav.	x			
Socratea exorrhiza (Mart.) H. Wendl.*	x			
Wettinia hirsuta Burret			x	x

*The types of plant parts sampled are shown. An *Indicates species that were used if Andean specimens were not available.*

RESULTS

All species and plant parts sampled produced abundant phytoliths, and contained one to four morphotypes (Table 2). We identified several new subtypes of globular echinate and conical morphotypes, which were previously characterized by other researchers (e.g., Piperno, 2006; Morcote-Ríos et al., 2016; Figure 1). The newly identified subtypes were defined by the following characteristics:

1. Globular echinate variant 1: Regularly arranged projections (Figure 1A). This globular echinate subtype contained clear projections that were roughly evenly distributed on the surface. Some variation in size and number of projections occurred, but they were always clearly visible and consistently shaped on the same phytolith. Size: 4–18 μm. This subtype was found in *Euterpe* and *Hyospathe* (Table 2). Photo: *Euterpe precatoria,* seed.

2. Globular echinate variant 2: Crowded projections (Figure 1B). This subtype appeared "hairy" due to its high density of projections. Individual projections were clear, with tapered ends, but the denser and seemingly chaotic coverage distinguished this type from variant 1 (Figure 1A). Size: 4–10 μm. This subtype was restricted to *Ceroxylon* (Table 2). Photo: *Ceroxylon alpinum,* woody parts.

3. Globular echinate variant 3: Irregular projections (Figure 1C). This subtype was distinguished by its irregularly shaped and arranged projections. They were

TABLE 2 | Percentages of phytolith morphotypes found within the plant parts sampled for Andean palm species.

	GE var. 1	GE var. 2	GE var.3	GE var. 4	LGG	GEE var. 1	GEE var. 2	RE var. 1	C var. 1	C var. 2	C var. 3	C var. 4+
TRIBE CEROXYLEAE												
Ceroxylon alpinum (leaf)		76.2				15.6	7.2	1.0				
Ceroxylon alpinum (seed)		100										
Ceroxylon alpinum (wood)		19.1		65.5		15.4						
TRIBE CHAMAEDOREEAE												
Chamaedorea pinnatifrons (leaf)										57.4	42.6	
TRIBE COCOSEAE												
Subtribe Bactridinae												
Aiphanes aculeata (wood)										54.1	45.9	
Bactris simplicifrons (leaf)									35.5	42.1	22.3	
Subtribe Euterpeae												
Euterpe precatoria (leaf)	12.5		75.7		4.5	7.3						
Euterpe precatoria (seed)	69.6			16.0		14.4						
Euterpe precatoria (wood)	70.0					17.7	12.3					
Euterpe catinga Wallace (leaf)	26.8		71.2		1.9							
Hyospathe elegans (leaf)	79.6					14.2	3.9	2.3				
Subtribe Geonomateae												
Geonoma paradoxa (leaf)							6.3					93.7
Geonoma undata (leaf)											54.6	45.4
Geonoma undata (wood)							14.7					85.3
TRIBE IRIARTEEAE												
Dictyocaryum fuscum (leaf)									100			
Dictyocaryum fuscum (seed)											100	
Iriartea deltoidea (leaf)									100			
Socratea exorrhiza (leaf)*									100			
Wettinia hirsuta (flower)										57.4	42.6	
Wettinia hirsuta (seed)										65.3	34.7	

*indicates species that were used if Andean specimens were not available. +indicates direct correspondence with the categories of Morcote-Ríos et al. (2016). GE, globular echinate; LGG, large globular granulate; GEE, globular echinate elongate; RE, reniform echinate; C, conical.

relatively few in number and of different sizes on the same phytolith, and irregularly placed on the surface, giving a starry rather than round overall appearance. Size: 4–15 μm. This subtype was only found in *Euterpe* (**Table 2**). Photo: *Euterpe precatoria,* leaf.

4. Globular echinate variant 4: Short, bold projections (**Figure 1D**). This subtype appeared similar to the "globular echinate with dense short projections" described by

Morcote-Ríos et al. (2016). It also appeared similar to the "large globular echinate" described by Dickau et al. (2013) and Watling et al. (2016), but smaller in size. This phytolith type contained many very small, bold projections. Due to the high number and stubby shape of the projections it did not have the typical thorny echinate outline. Size: 6–14 μm. This subtype was found in *Ceroxylon* and *Euterpe* (**Table 2**). Photo: *Ceroxylon alpinum,* wood.
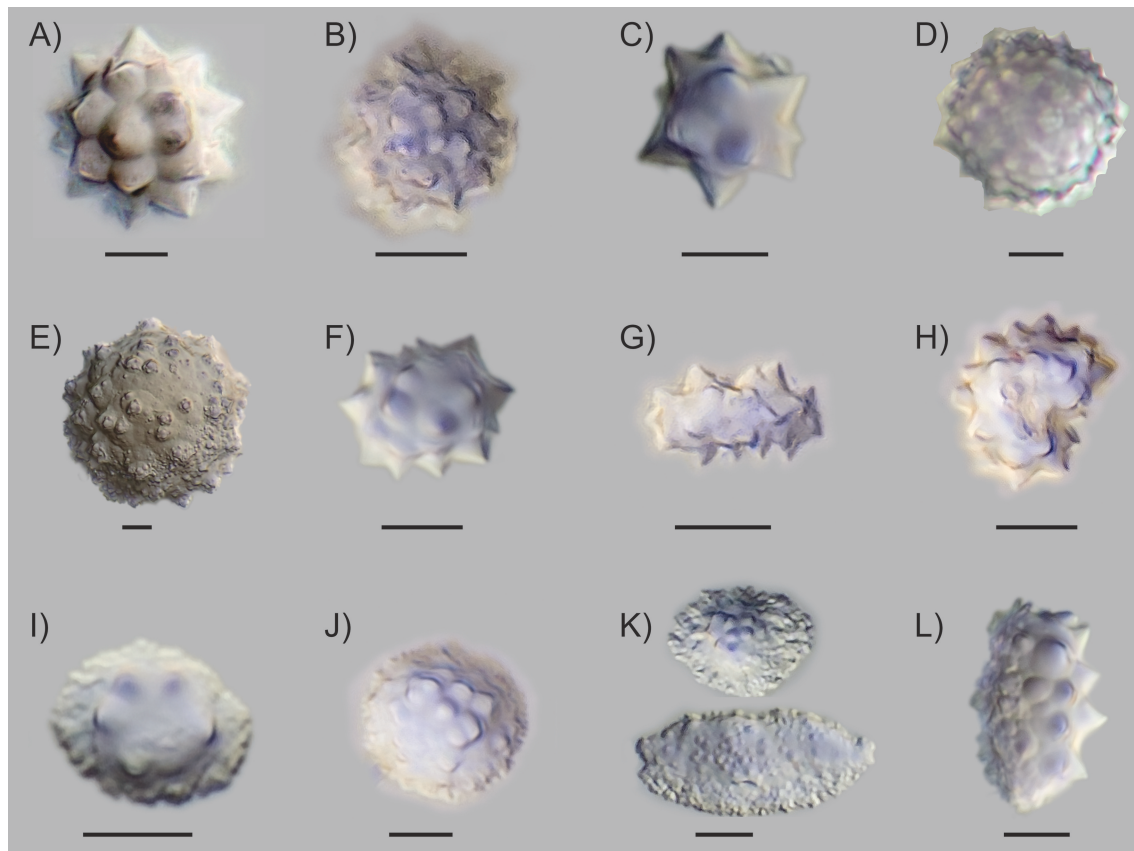
FIGURE 1 | Phytolith morphotypes identified from herbarium material of species that are found in mid-elevation Andean forests **(A)** globular echinate variant 1: regularly arranged projections; **(B)** globular echinate variant 2: crowded projections; **(C)** globular echinate variant 3: irregular projections; **(D)** globular echinate variant 4: short, bold projections; **(E)** large globular granulate; **(F)** globular echinate elongate variant 1: elliptical; **(G)** globular elongate variant 2: straight; **(H)** reniform echinate variant 1: thick; **(I)** conical variant 1: few (3–6) projections arranged around the top; **(J)** conical variant 2: many (8–20) projections arranged densely on top; **(K)** conical variant 3: flat or plateaued, projections arranged randomly on top surface; **(L)** conical variant 4: with basal projections. The scale bar for each phytolith is 5 μm in length.

5. Large globular granulate (**Figure 1E**). This type was clearly distinguished by its significantly larger size and surface ornamentation. Its projections were very short and of different shapes, all very granulate and often with multiple small mounds on top or in between. They were unevenly distributed across the surface of the phytolith. Due to the granulate and unsharp character of the projections we did not name this type "echinate." It was more similar in size though had different projections than the previously described "large globular echinate" (Dickau et al., 2013; Watling et al., 2016). Size: 18–38 μm. It was a relatively rare type among the other echinate variants, but easy to recognize and therefore very diagnostic. This subtype was only found in leaves of *Euterpe* (**Table 2**). Photo: *Euterpe precatoria*, leaf.

6. Globular echinate elongate variant 1: elliptical (**Figure 1F**). This elongated echinate had an oval shape with curved sides. Some were more elongated than others, but they always presented curved sides accounting for the elliptical shape. Length axis: 7–17 μm. This subtype was found in *Ceroxylon, Euterpe,* and *Hyospathe* (**Table 2**). In *Ceroxylon,*

the projections were generally shorter than in *Hyospathe* and *Euterpe*. Photo: *Euterpe precatoria*, wood.

7. Globular echinate elongate variant 2: straight (**Figure 1G**). The elongated sides of this variant were straight, as opposed to the curved sides of variant 1 (**Figure 1F**). This gave a more long, stretched, and bar-like overall shape. This variant contained well-pronounced, irregularly distributed projections. Length axis: 6–14 μm. This subtype was abundant in *Hyospathe* and found in fewer numbers in the woody parts of *Euterpe* (**Table 2**). Photo: *Hyospathe elegans,* leaf.

8. Reniform echinate variant 1: thick (**Figure 1H**). This subtype was a curved echinate. The curviness and thickness varied per phytolith, but they were much thicker and mostly bigger than the reniform type described by Morcote-Ríos et al. (2016). Longest axis: 4–16 μm. This subtype was found in *Ceroxylon*, *Hyospathe,* and *Geonoma*, although less frequently in *Geonoma* (**Table 2**). Photo: *Hyospathe elegans,* leaf.

9. Conical variant 1: few (3–6) projections arranged around the top (**Figure 1I**). This conical phytolith had the typical conical

overall shape. Its projections were few in number (3–6), and they were arranged around the top in a roughly circular arrangement. In most cases the projections were pronounced and easily discernible. Diameter/base length: 5–18 µm. This subtype was found in *Bactris, Dictyocaryum, Iriartea,* and *Socratea* (**Table 2**). In *Dictyocaryum* and *Socratea*, sizes were fairly consistent, with ca. 10 and 15 µm base length, respectively. *Iriartea* sizes were consistently 15–18 µm, and *Bactris* presented highly variable sizes. Photo: *Dictyocaryum fuscum,* leaf.

10. Conical variant 2: many (8–20) projections arranged densely on top (**Figure 1J**). This conical subtype had more projections (8–20) than the former subtype, which were arranged densely on the top of the phytolith. In some cases, the projections were pronounced and easily discernible despite being densely packed, but in other cases they were blunter. The overall shape could be round, with a very gradual transition to the top part containing the projections (as in **Figure 1J**), but also elongated. In that case the bottom part could be extensively elongated and relatively flat, with the elevated top part being reduced to a small, bulblike arrangement of projections (**Figure S1**). Diameter/base length: 7–24 µm. This subtype was found in *Chamaedorea, Aiphanes, Bactris,* and *Wettinia* (**Table 2**). *Bactris simplicifrons* presented very round, high, pointy bodies that were larger than found in other species with this subtype (18–24 µm). In *Chamaedorea,* this subtype had a consistent size of ca. 10 µm and was not as pointy, but rather round in overall shape. *Chamaedorea* and *Aiphanes* showed more variation within this subtype. Photo: *Chamaedorea pinnatifrons,* leaf.

11. Conical variant 3: flat or plateaued, projections arranged randomly on top surface (**Figure 1K**). This subtype hardly showed a conical shape, and its overall form was flat or plateau-like. It was often elongated, but in contrast to the former described subtype, it did not possess the bulblike, elevation top part with projections. Instead, it often showed smaller, bold, randomly placed projections on the top surface. In some cases, the projections were centered in a slightly elevated part or appeared seemingly ridge-like on top of an elongated body. In other cases, the projections occurred on top of a flat overall appearing body. The bottom often looked crumbly or crenate and showed many different shapes, contributing to the high overall variation. Due to its often very small projections and hardly conical shape, this type tended to resemble rugose spheres, which represent arboreal taxa (Piperno, 2006). Diameter/base length: 4–15 µm. This subtype was found in *Chamaedorea, Aiphanes, Bactris, Geonoma, Dictyocaryum,* and *Wettinia* (**Table 2**). Photo: *Wettinia hirsuta,* seed.

12. Conical variant 4: with basal projections (**Figure 1L**). This subtype resembled the conical with basal projections type as described by Morcote-Ríos et al. (2016). Its multiple projections extended to the base of the phytolith, thereby covering the entire half of the phytolith. The bottom was similar to other conical variants or appeared jagged compared with other variants. Diameter/base length:

6–15 µm. This subtype was restricted to *Geonoma*. Photo: *Geonoma paradoxa,* leaf.

Most samples contained multiple phytolith subtypes, and there was variation of subtypes within and between species (**Table 2**). The *Ceroxylon alpinum* samples produced one or more of the globular echinate or reniform subtypes (**Table 2**). The seed samples, however, produced only globular echinate variant 2. The Cocoseae tribe samples also contained the globular echinate and reniform subtypes, but only in the Euterpeae and Geonomateae subtribes (**Table 2**). The leaves of *Euterpe* produced predominantly globular echinate variant 3, which was absent in *Ceroxlyon alpinum*. *Euterpe* seed and wood samples, and *Hyospathe elegans* leaf samples, had assemblages dominated by globular echinate variant 1 (**Table 2**). Reniform phytoliths occurred in low abundances in *Hyospathe elegans* and *Geonoma* samples (**Table 2**).

Conical phytoliths occurred primarily in the Iriarteeae and Chamaedoreeae tribes, and the Bactridinae and Geonomatae subtribes of the Cocoseae (**Table 2**). Leaf samples from *Dictyocaryum*, *Iriartea*, and *Socratea* contained 100% conical variant 1 phytoliths. *Bactris simplicifrons* also contained conical variant 1 phytoliths, but in lower abundances (**Table 2**). *Chamaedorea pinnatifrons*, *Aiphanes aculeata*, *Bactris simplicifrons*, and *Wettinia hirsuta* contained conical variant 2 phytoliths. Those same species, *Geonoma undata*, and *Dictyocaryum fuscum* (seeds only) contained conical variant 3 phytoliths (**Table 2**). Conical variant 4 phytoliths were produced primarily by *Geonoma* (**Table 2**).

DISCUSSION

We defined several new subdivisions among the most recently described globular echinate and conical palm phytolith morphotypes (Morcote-Ríos et al., 2016; **Figure 1**). Our subdivided morphotype categories were based on DIC microscopy using 630x magnification, which was necessary to characterize differences within the broader globular echinate and conical categories, particularly when the phytoliths were ca. 10 µm or smaller (**Figure 1**). Even with this magnification, it can still be difficult to distinguish surface ornamentation on some of these small phytoliths. We suggest that future identifications of palm phytoliths should be performed using a minimum magnification of 630x, but preferably a magnification of 1,000x. Scanning electron microscopy can also be particularly useful at identifying the nuances of phytolith morphotypes (Bowdery, 2015), though this approach is much more time consuming and may not be feasible when examining more than 250 phytoliths per sample and tens to hundreds of samples per sediment core.

The angle of view can also complicate identification of a single phytolith, especially in fossil samples. Silica-based microfossils are often mounted solidly and cannot be rotated once the mounting solution has dried, which fixes the angle of view. Our observations from the herbarium specimens of *Geonoma* indicated that the conical with basal projections type can resemble a globular echinate when viewed straight from the top,

but it can also appear as an arboreal rugose sphere if positioned upside-down (**Figure S2**). The reference material from *Euterpe precatoria* and *E. catinga* also indicated that symmetry, a feature that was earlier used to distinguish echinate types (Morcote-Ríos et al., 2016), might be hard to determine when the phytoliths dry at different angles in the mounting solution (**Figure S3**). We therefore suggest to allow for rotation of the phytoliths by analyzing the slides before the mounting solution has fully dried, as we partly did in this study, or by using a non-solidifying mounting medium such as liquid Entellan, glycerine or immersion oil (Cabanes and Shahack-Gross, 2015). However, the refractive indices of these media are similar to phytoliths and can make their overall features less distinguishable (Piperno, 2006). Because symmetry exists along a gradient, and identifying symmetry can also be troubled by damage or deterioration of the phytoliths in fossil samples, we did not include it as a diagnostic feature in our categorization.

Though we have classified new subtypes of phytoliths, the examination of the herbarium material suggested that phytolith morphologies occur as a gradient as opposed to clearly defined differences in types. For example, the newly characterized conical variants presented here are named "conical" following the previously described general category, which has also been called hat-shaped in some literature (Piperno, 2006; Tomlinson et al., 2011; Morcote-Ríos et al., 2016). Our examination of the conical phytoliths, however, revealed that the conical variants 2 and 3 do not always exhibit a true conical shape, and can also exhibit a range of shapes on their base (**Figures 1I–K**, **Figure S1**). These variations are mostly found in *Chamaedorea*, *Aiphanes*, and *Wettinia* (**Table 2**). The flowers of *Wettinia hirsuta* in particular exhibited a wide variation in shapes of the conical base and in the configuration of projections.

There seems to be a particularly strong gradient in the reniform echinate phytoliths, which ranged from small, thin and highly curved specimens (**Figure S4**) to large, thick and minimally curved ones (**Figure 1H**). *Ceroxylon*, *Hyospathe*, and *Geonoma* contained thick reniform shapes, which we identified as reniform echinate variant 1 (**Table 2**). The smaller, thinner reniform shapes described by Morcote-Ríos et al. (2016) were very rare in our samples, and we suggest those should be considered a different variant (i.e., reniform variant 2). We encountered a few thin reniform-like shapes in the leaves of *Geonoma paradoxa;* however, some of them appeared more randomly kinked than evenly curved and resembled caterpillar shapes (**Figure S4**). We are therefore uncertain if these "caterpillar" reniform phytoliths should be considered a separate variant (e.g., reniform variant 3), but we have also encountered them in fossil samples. Future studies focused on these reniform echinate phytoliths will be able to further determine subdivisions.

Geonoma was the only palm genus where conical and reniform echinate phytoliths co-occurred in the same sample. *Geonoma* was also the only genus where previous studies have reported the rare co-occurrence of conical phytolith with non-conical types (Tomlinson et al., 2011; Morcote-Ríos et al., 2016). In both of those cases, the co-occurrence happened with an echinate subtype that we did not encounter in our samples. We very rarely encountered echinate and conical types in the same

phytolith sample apart from in *Geonoma* samples, and did not include these exceptions in **Table 2** because the echinates were so rare and we cannot rule out the possibility of contamination of the herbarium sheets that we sampled. Even though *Geonoma* produced an array of phytolith subtypes, it was the only genus to produce high amounts of conical variant 4 phytoliths (**Table 2**). Thus, in eastern Andean forests, high amounts of conical variant 4 phytoliths likely represent *Geonoma*, a genus of primarily understory palms whose Andean species grow larger than their lowland counterparts (up to 12 cm diameter and 13 m height) (Moraes et al., 1995). Andean *Geonoma* species are also economically important (e.g., Bernal et al., 2011), so the presence or absence of *Geonoma* phytoliths from archaeological settings may provide information on its past use and dispersal.

In many samples we encountered individual phytoliths that appeared deformed. This occurred primarily in seeds and woody parts, and much less frequently in leaf samples. Deformations ranged from completely randomly shaped bodies (e.g., wood/seeds of *Ceroxylon alpinium*, *Euterpe precatoria,* and *Geonoma*) (**Figure S5**) to still recognizable diagnostic types with smaller deformations, e.g., conical phytoliths that were extensively elongated or "tailed" at the base in *Dictyocaryum* seeds (**Figure S6**). We did not examine the ratios of the deformed phytoliths within samples, primarily because these ratios would not be applicable in a paleoecological or archaeological context where all phytoliths are intermixed.

Ceroxylon is one of the only palm genera that is more common at higher elevations (i.e., >2,000 masl) than at lower elevations (Moraes et al., 1995). *Ceroxylon* produced primarily globular echinate phytoliths and fewer reniform echinate phytoliths, as did some of the Euterpeae, which typically grow at lower elevations (Moraes et al., 1995; **Table 2**). *Ceroxylon*, however, was the only species to produce the globular echinate variant 2 phytoliths (**Table 2**, **Figure 1B**). Thus, the globular echinate variant 2 phytoliths in paleoecological contexts can be used to identify *Ceroxylon*, and indicate colder conditions than most other palm species prefer. *Ceroxylon* is also an economically important plant species (e.g., Bernal et al., 2011), and its phytoliths (or the absence of them) can now also be used in archaeological settings to reconstruct past palm management practices and the dispersal of economically important taxa. *Ceroxylon* also produced other types of unique silica structures that were not found in any other species that we sampled (**Figure S7**). These silica structures may come from the "waxy wood" that has commonly been described in *Ceroxylon*, which does not occur in most palm species (Moraes et al., 1995).

Size variation can be a key distinguishing feature in phytolith identification. In the case of *Wettinia hirsuta*, the variation of phytoliths between plant parts was mostly in terms of size. The seeds produced ca. 2–6 μm larger phytoliths than the flower. Perhaps more importantly for paleoecological and archaeological reconstructions, we found that the size variation of phytolith subtypes can be used to distinguish species from each other. For example, *Iriartea deltoidea* and *Dictyocaryum lamarckianum* produce 100% the same subtype of conical variant 1 in their leaves. The phytoliths produced by *Iriartea*, however, are consistently and significantly larger than those produced by

Dictyocaryum. Conical phytoliths from *Iriartea* typically range from 15 to 18 μm, whereas those found in *Dictyocaryum* range from 5 to 10 μm. *Iriartea deltoidea* is one of the most common trees in the Amazonian lowlands (Pitman et al., 2001; ter Steege et al., 2013), and rarely exceeds 1,300 masl (Henderson et al., 1997). In contrast, *Dictyocaryum* ranges primarily from 1,000 to 2,000 masl (Moraes et al., 1995). The ability to distinguish the conical phytoliths of these two species is therefore particularly advantageous in reconstructions of past climatic conditions.

Our newly characterized palm phytolith types (**Figure 1**, **Table 2**) provide a foundation to identify palm genera with narrow altitudinal ranges in mid-elevational Andean settings. Mid-elevation Andean ecosystems are some of the most diverse and threatened ecosystems on Earth (Olson et al., 2001; Olson and Dinerstein, 2002), and past climatic change has helped shape these systems into their current configuration (e.g., Flenley, 1979; Bush, 2002; Bush et al., 2007). Identification of an increased number of Andean palm phytolith subtypes, and the increased ability to associate them with a specific palm genus or set of genera, can provide more detailed reconstructions of past ecological dynamics in paleoecological and archaeobotanical contexts than was previously possible. Because phytoliths reflect local-scale vegetation dynamics (e.g., Piperno, 2006), ecological responses to past climatic changes or human activity can also be reconstructed at a higher spatial resolution than when using only pollen data. If paired, pollen and phytolith analyses could be used to determine regional vs. local vegetation change in Andean settings, as has been done in the Amazonian lowlands (e.g., Carson et al., 2014).

CONCLUSIONS

Mid-elevation Andean forests are some of Earth's most diverse and threatened ecosystems, yet their ecological history remains understudied. Phytoliths, which represent local-scale vegetation, are a valuable tool in reconstructing vegetation dynamics through time. Our study provides a more nuanced categorization of palm phytoliths than was previously available, and also demonstrates their potential to create more comprehensive paleoecological reconstructions of local-scale

vegetation dynamics than previously possible. Phytoliths are becoming much more commonly used in paleoecological and archaeological reconstructions because of their potential in reconstructing local-scale vegetation patterns, and we stress the need to continue referencing regionally-specific palm (and also arboreal) phytoliths.

DATA AVAILABILITY STATEMENT

The phytolith reference material generated for this study can be found in the phytolith reference collection at the University of Amsterdam.

AUTHOR CONTRIBUTIONS

FUNDING

ACKNOWLEDGMENTS

SUPPLEMENTARY MATERIAL

The Supplementary Material for this article can be found online at: https://www.frontiersin.org/articles/10.3389/fevo.2018.00193/full#supplementary-material

REFERENCES

Bernal, R., Torres, C., García, N., Isaza, C., Navarro, J., Vallejo, M. I., et al. (2011). Palm management in South America. *Bot. Rev.* 77, 607–646. doi: 10.1007/s12229-011-9088-6

Bowdery, D. (2015). An enigma revisited: identification of palm phytoliths extracted from the 1983 Rapa Nui, Rano Kao2 core. *Veg. Hist. Archaeobot.* 24, 455–466. doi: 10.1007/s00334-014-0503-x

Bush, M. B. (2002). Distributional change and conservation on the Andean flank: a palaeoecological perspective. *Glob. Ecol. Biogeogr.* 11, 463–467. doi: 10.1046/j.1466-822X.2002.00305.x

Bush, M. B., Hanselman, J. A., and Hooghiemstra, H. (2007). "Andean montane forests and climate change," in *Tropical Rainforest Responses to Climatic Change,* eds M. B. Bush and J. R. Flenley (Heidelberg: Springer), 33–54. doi: 10.1007/978-3-540-48842-2_2

Bush, M. B., Hanselman, J. A., and Hooghiemstra, H. (2011). "Andean montane forests and climate change," in *Tropical Rainforest Responses to Climate Change 2nd Edn,* eds M. B. Bush and J. R. Flenley (Chichester: Praxis Springer), 35–60. doi: 10.1007/978-3-642-05383-2_2

Bush, M. B., Hansen, B. C. S., Rodbell, D., Seltzer, G. O., Young, K. R., León, B., et al. (2005). A 17,000 year history of Andean climatic and vegetation change from Laguna de Chochos, Peru. *J. Q. Sci.* 20, 703–714. doi: 10.1002/jqs.983

Cabanes, D., and Shahack-Gross, R. (2015). Understanding fossil phytolith preservation: the role of partial dissolution in paleoecology and archaeology. *PLoS ONE* 10:e0125532. doi: 10.1371/journal.pone.0125532

Carson, J. F., Whitney, B. S., Mayle, F. E., Iriarte, J., Prümers, H., Soto, J. D., et al. (2014). Environmental impact of geometric earthwork construction in pre-Columbian Amazonia. *Proc. Natl Acad. Sci. U.S.A.* 111, 10497–10502. doi: 10.1073/pnas.1321770111

Dickau, R., Whitney, B. S., Iriarte, J., Mayle, F. E., Soto, J. D., Metcalfe, P., et al. (2013). Differentiation of neotropical ecosystems by modern soil phytolith assemblages and its implications for palaeoenvironmental and archaeological reconstructions. *Rev. Palaeobot. Palynol.* 193, 15–37. doi: 10.1016/j.revpalbo.2013.01.004

Flenley, J. (1979). The late quaternary vegetational history of the equatorial mountains. *Prog. Phys. Geogr.* 3, 488–509. doi: 10.1177/030913337900300402

Gnecco, C. (2003). Against ecological reductionism: late pleistocene hunter-gatherers in the tropical forests of northern South America. *Q. Int.* 109, 13–21. doi: 10.1016/S1040-6182(02)00199-4

Henderson, A., Galeano-Garces, G., and Bernal, R. (1997). *Field Guide to the Palms of the Americas*. Princeton, NJ: Princeton University Press.

Kahn, F., and De Granville, J.-J. (2012). *Palms in Forest Ecosystems of Amazonia*. Berlin: Springer Science and Business Media.

Kahn, F., and Mejia, K. (1990). Palm communities in wetland forest ecosystems of Peruvian Amazonia. *For. Ecol. Manage.* 33, 169–179. doi: 10.1016/0378-1127(90)90191-D

Mora, S., and Camargo, S. M. (2003). *Early Inhabitants of the Amazonian Tropical Rain Forest: A Study of Humans and Environmental Dynamics*. Pittsburgh, PA: Department of Anthropology, University of Pittsburgh.

Moraes, M., Galeano, G., Bernal, R., Balslev, H., and Henderson, A. (1995). "Tropical Andean palms (Arecaceae)," in *Biodiversity and Conservation of Neotropical Montane Forest,* eds S. P. Churchill, H. Balslev, E. Forero, and J. L. Luteyn (New York, NY: New York Botanical Garden), 473–487.

Morcote-Rios, G., and Bernal, R. (2001). Remains of palms (Palmae) at archaeological sites in the new world: a review. *Bot. Rev.* 67, 309–350. doi: 10.1007/BF02858098

Morcote-Ríos, G., Bernal, R., and Raz, L. (2016). Phytoliths as a tool for archaeobotanical, palaeobotanical and palaeoecological studies in Amazonian palms. *Bot. J. Linn. Soc.* 182, 348–360. doi: 10.1111/boj.12438

Olson, D. M., and Dinerstein, E. (2002). The Global 200: priority ecoregions for global conservation. *Ann. Miss. Bot. Gardens* 89, 199–224. doi: 10.2307/3298564

Olson, D. M., Dinerstein, E., Wikramanayake, E. D., Burgess, N. D., Powell, G. V. N., Underwood, E. C., et al. (2001). Terrestrial ecoregions of the world: a new map of life on earth. *Bioscience* 51, 933–938. doi: 10.1641/0006-3568(2001)051[0933:TEOTWA]2.0.CO;2

Phillips, O., and Miller, J. S. (2002). *Global Patterns of Plant Diversity: Alwyn H. Gentry's Forest Transect Data Set*. St. Louis, MI: Missouri Botanical Press.

Piperno, D. R. (2006). *Phytoliths: A Comprehensive Guide for Archaeologists and Paleoecologists*. Lanham, MD: Alta Mira Press.

Piperno, D. R., and Sues, H. D. (2005). Dinosaurs dined on grass. *Science* 310, 1126–1128. doi: 10.1126/science.1121020

Pitman, N. C. A., Terborgh, J. W., Silman, M. R., Nunez, P. V., Neill, D. A., Cerón, C. E., et al. (2001). Dominance and distribution of tree species in upper Amazonian terra firme forests. *Ecology* 82, 2101–2117. doi: 10.1890/0012-9658(2001)082[2101:DADOTS]2.0.CO;2

Prasad, V., Strömberg, C. A., Alimohammadian, H., and Sahni, A. (2005). Dinosaur coprolites and the early evolution of grasses and grazers. *Science* 310, 1177–1180. doi: 10.1126/science.1118806

Schiferl, J. D., Bush, M. B., Silman, M. R., and Urrego, D. H., (2017). Vegetation responses to late Holocene climate changes in an Andean forest. *Q. Res.* 89, 60–74. doi: 10.1017/qua.2017.64

Smith, N. (2014). *Palms and People in the Amazon*. Heidelberg: Springer.

Strömberg, C. A. (2004). Using phytolith assemblages to reconstruct the origin and spread of grass-dominated habitats in the great plains of North America during the late Eocene to early Miocene. *Palaeogeogr. Palaeoclimatol. Palaeoecol.* 207, 239–275. doi: 10.1016/j.palaeo.2003.09.028

Strömberg, C. A., and McInerney, F. A. (2011). The Neogene transition from C3 to C4 grasslands in North America: assemblage analysis of fossil phytoliths. *Paleobiology* 37, 50–71. doi: 10.1666/09067.1

ter Steege, H., Pitman, N. C. A., Sabatier, D., Baraloto, C., Salomão, R. P., Guevara, J. E., et al. (2013). Hyperdominance in the Amazonian tree flora. *Science* 342:1243092. doi: 10.1126/science.1243092

Tomlinson, P. B., Horn, J. W., and Fisher, J. B. (2011). *The Anatomy of Palms: Arecaceae-Palmae*. Oxford, UK: OUP Oxford. doi: 10.1093/acprof:osobl/9780199558926.001.0001

Vormisto, J., Tuomisto, H., and Oksanen, J. (2004). Palm distribution patterns in Amazonian rainforests: What is the role of topographic variation? *J. Veg. Sci.* 15, 485–494. doi: 10.1111/j.1654-1103.2004.tb02287.x

Watling, J., Iriarte, J., Whitney, B., Consuelo, E., Mayle, F., Castro, W., et al. (2016). Differentiation of neotropical ecosystems by modern soil phytolith assemblages and its implications for palaeoenvironmental and archaeological reconstructions II: southwestern Amazonian forests. *Rev. Palaeobot. Palynol.* 226, 30–43. doi: 10.1016/j.revpalbo.2015.12.002